Surface Reactions

International Edition: DOI: 10.1002/anie.201602859
German Edition: DOI: 10.1002/ange.201602859

On-Surface Domino Reactions: Glaser Coupling and Dehydrogenative Coupling of a Biscarboxylic Acid To Form Polymeric Bisacylperoxides

Philipp Alexander Held, Hong-Ying Gao, Lacheng Liu, Christian Mück-Lichtenfeld, Alexander Timmer, Harry Mönig, Dennis Barton, Johannes Neugebauer, Harald Fuchs,* and Armido Studer**

Dedicated to Professor Gerhard Erker on the occasion of his 70th birthday

Abstract: *Herein we report the on-surface oxidative homocoupling of 6,6′-(1,4-buta-1,3-diynyl)bis(2-naphthoic acid) (BDNA) via bisacylperoxide formation on different Au substrates. By using this unprecedented dehydrogenative polymerization of a biscarboxylic acid, linear poly-BDNA with a chain length of over 100 nm was prepared. It is shown that the monomer BDNA can be prepared in situ at the surface via on-surface Glaser coupling of 6-ethynyl-2-naphthoic acid (ENA). Under the Glaser coupling conditions, BDNA directly undergoes polymerization to give the polymeric peroxide (poly-BDNA) representing a first example of an on-surface domino reaction. It is shown that the reaction outcome varies as a function of surface topography (Au(111) or Au(100)) and also of the surface coverage, to give branched polymers, linear polymers, or 2D metal–organic networks.*

The emerging research area of on-surface synthesis, which allows preparing well-defined, covalently connected nanostructures on surfaces, has received much attention in recent years.[1–5] Various on-surface reactions, such as the Ullmann coupling,[6–11] imine formation,[12–14] condensation of boronic acids,[15] carbene dimerization,[16] cycloadditions,[17–20] and dehydrogenation reactions[8,21–25] have been developed. The noble-metal surface as a novel type of reaction medium offers reactivities, that are not accessible in solution phase chemistry, as convincingly documented by the reported linear alkane polymerization via C–H activation on Au(110).[26]

[*] P. A. Held, Dr. C. Mück-Lichtenfeld, D. Barton, Prof. Dr. J. Neugebauer, Prof. Dr. A. Studer
Organisch-Chemisches Institut
Westfälische Wilhelms-Universität Münster
Corrensstrasse 40, 48149 Münster (Germany)
E-mail: studer@uni-muenster.de
Dr. H.-Y. Gao, L. Liu, A. Timmer, Dr. H. Mönig, Prof. Dr. H. Fuchs
Physikalisches Institut
Westfälische Wilhelms-Universität Münster
Wilhelm-Klemm-Strasse 10, 48149 Münster (Germany)
and
Center for Nanotechnology (CeNTech)
Heisenbergstrasse 11, 48149 Münster (Germany)
E-mail: gaoh@uni-muenster.de
fuchsh@uni-muenster.de

Supporting information for this article can be found under: http://dx.doi.org/10.1002/anie.201602859.

Along with the most commonly applied aryl halides or alkynes as building blocks, compounds bearing carbonyl groups as reactive functionalities have been used in on-surface chemistry owing to their versatility in classical organic synthesis.[27–30] Self-assembled nanostructures of aromatic carboxylic acids on metal surfaces have been intensively investigated because of their ability to form self-complementary hydrogen bonds and strong interactions with the metal substrate.[31–33] It has also been reported that these interactions can be further increased by formation of carboxylates via deprotonation.[31] In fact, carboxylic acids have been amply used for preparation of diverse metal–organic coordination networks (mainly via co-depositing acids with metal atoms onto the surface).[34–36] However, despite these intensive efforts, the only known on-surface reaction comprising the carboxylic acid functionality in covalent bond formation is our previously reported polymerization of 2,6-naphthalenedicarboxylic acid via decarboxylative C–C bond formation.[37]

Herein, we disclose a new type of a surface-mediated chemical reaction of the carboxyl acid functionality: we show that the aromatic acid 6-ethynyl-2-naphthoic acid (ENA) reacts via Glaser coupling and subsequent dehydrogenative coupling of the acid moiety to give the corresponding polymeric bisacylperoxide in a domino reaction.[38,39] This remarkable on-surface sequence allows preparing long polymer chains with a bisacylperoxide connection motif under ultrahigh vacuum (UHV) conditions (Scheme 1). Notably, the dehydrogenative coupling of acids is unknown in solution-phase chemistry, in which peroxides are generally used as stoichiometric oxidants in metal-nanoparticle catalysis. We will also show that the substrate topography, Au(111) versus Au(100), and the surface coverage allow controlling the reaction outcome.

Our initial experiments were performed on the Au(111) surface by using ENA as a monomer. ENA was selected because we attempted an orthogonal reaction sequence by in situ preparation of our desired building block unit, the 6,6′-(1,4-buta-1,3-diynyl)bis(2-naphthoic acid) (BDNA), directly at the surface via preceding Glaser coupling.[22] After depositing a submonolayer of ENA (ca. 40% surface coverage) the scanning tunneling microscopy (STM) data revealed the formation of a self-assembled structure confined by the Au(111) herringbone reconstruction and driven by hydrogen bonding of the acid groups as well as van der Waals interactions between the aromatic backbones (Figure 1a).

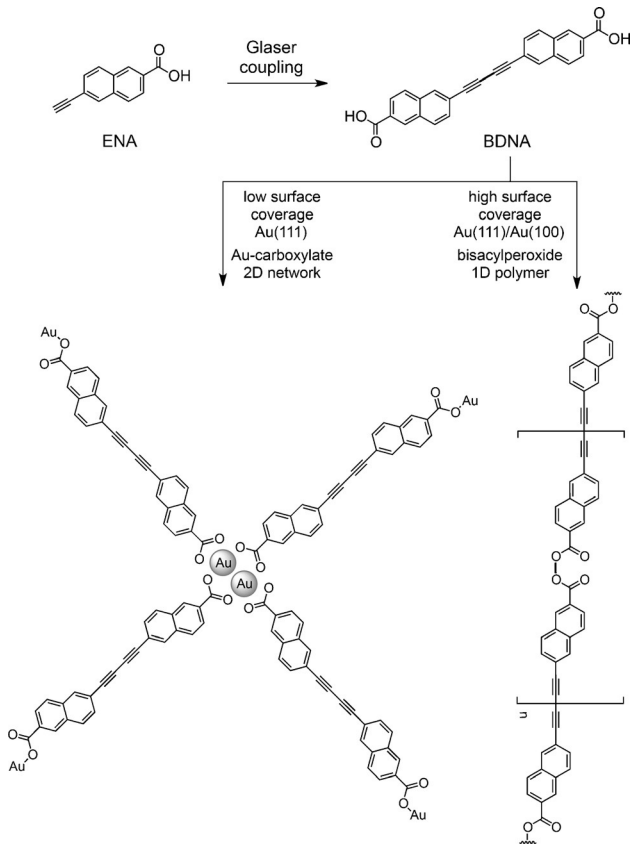

Scheme 1. Illustration of the on-surface reaction process of ENA for poly(bisacylperoxide) and gold carboxylate formation, controlled by the surface topography and coverage.

Subsequent annealing to 124 °C allowed for dehydrogenative dimerization of the terminal alkyne functionalities (Glaser coupling) and led to the formation of the BDNA units, which then further reacted to form a two-dimensional coordination network (Figure 1b). We assume Au carboxylates as the predominating connection motives formed during the annealing process. The experimentally determined naphthyl center-to-center distance of the coordination bridge was measured as 1.22 ± 0.04 nm and 1.49 ± 0.03 nm (L_a and L_b, Figure 1b-iii). These results and also the contrast signature of the frameworks are in good agreement with those reported for similar metal–carboxylate coordination networks, where co-deposited Fe or Ni atoms were used.[35,36]

Next we investigated the reaction under high coverage conditions. To this end, a close to one monolayer of ENA monomers was grown on the Au(111) crystal (Figure 2a). Subsequent annealing of the substrate to 124 °C resulted in the formation of two different phases, an ordered self-assembly region surrounded by a disordered phase of branched polymer chains (Figure 2b). STM investigations revealed that the ordered region consists of an intermediate state in the on-surface alkyne homocoupling, where an Au atom is pulled out of the surface and forms a linear bis-(alkinyl) gold complex with two ENA units connected by an Au atom (Figure 2b right close-up view). The measured distance between the naphthyl centers of this intermediate organometallic species was 1.43 ± 0.01 nm, which agrees very well with the theoretical distance (1.421 nm) calculated for a bis(alkinyl) Au complex (Figure S1 in the Supporting Information). Reductive elimination then provides the Glaser product. However, the expected primary product of the Glaser coupling reaction—the BDNA monomer—could not be identified in the STM images. Instead we found that once the Glaser coupling had occurred, the in situ formed BDNA molecules underwent fast follow up reactions. Based on the images we assumed that some acids reacted via an unprecedented dehydrogenative coupling leading to bisacylperoxide connected polymers (see below). These polymers can be identified in the disordered phase containing branched polymer chains. The branching points (indicated by red circles in Figure 2) exhibit the same gap size as the connection motif in the previously observed network under low coverage conditions and can therefore be considered as similar Au–carboxylate conjugations representing the second follow-up reaction of the acid

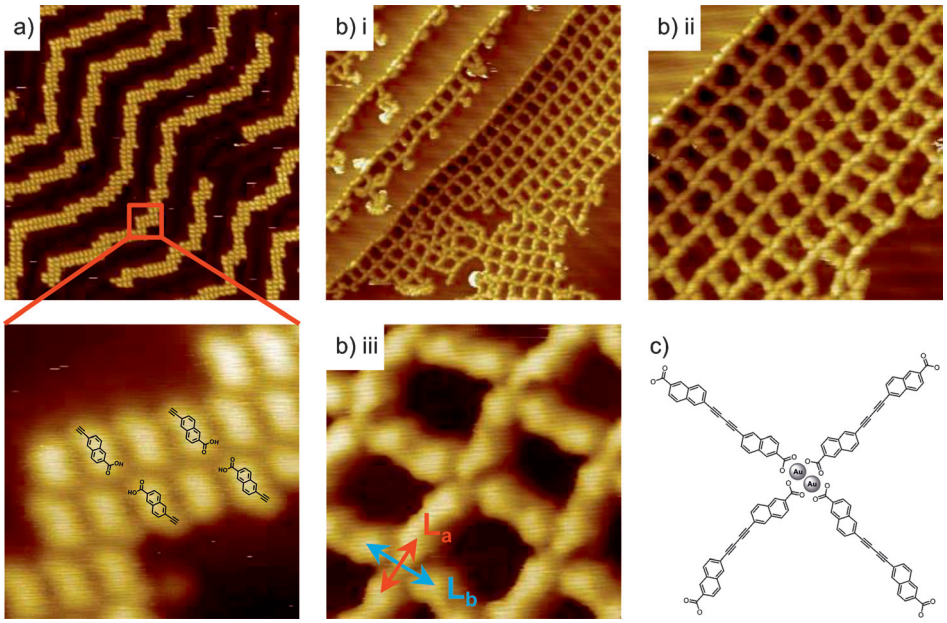

Figure 1. a) Overview STM image of the residual ENAs at sub-monolayer (ca. 40%) coverage (−2 V, 10 pA, 42 nm × 42 nm), with a high resolution image (−2 V, 10 pA, 4.2 nm × 4.2 nm). b) STM image of the 2D metal–organic polymers as reaction products after annealing at 124 °C. b-i) Overview image (−1 V, 10 pA, 42 nm × 42 nm), as well as high resolution images b-ii) the ordered structure of the 2D network (−1 V, 10 pA, 21 nm × 21 nm) and b-iii) conjunction shape inside the network (−1 V, 50 pA, 5.9 nm × 5.9 nm). c) Chemical structure of the Au carboxylate complex. All images were obtained on Au(111).

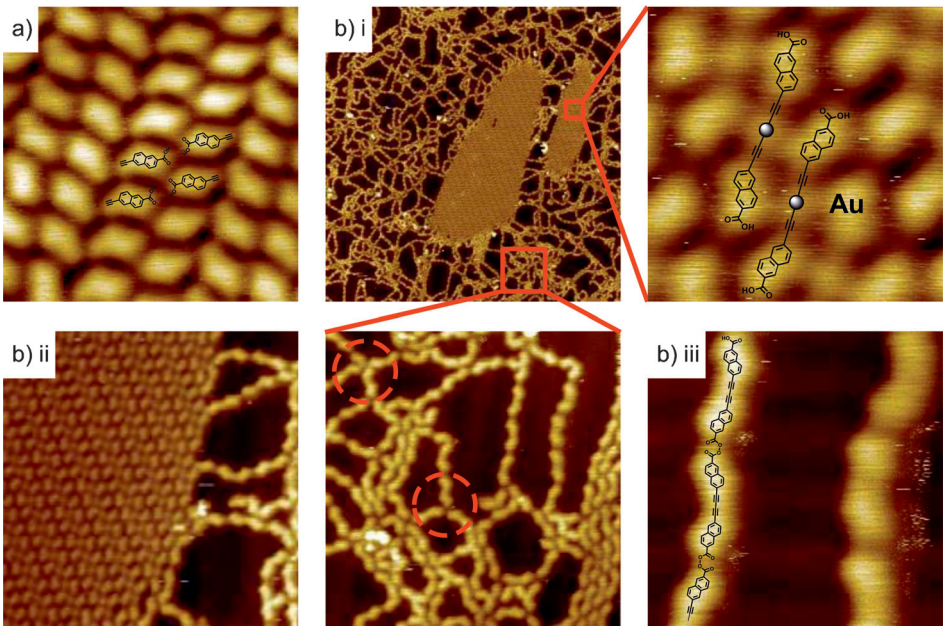

Figure 2. a) STM image of the residual ENAs at close to one monolayer coverage (−2 V, 50 pA, 5 nm × 5 nm). b) Reaction products after annealing to 124 °C. b-i) Overview image of all reaction products (−2 V, 5 pA, 72 nm × 72 nm), with close-up views, right: high-resolution image of an Au complex intermediate state of the Glaser coupling (−2 V, 20 pA, 2.6 nm × 2.6 nm), below: STM image of the disordered polymer chains (−2 V, 5 pA, 17 nm × 17 nm), b-ii) STM image of the border between the two product phases (−2 V, 20 pA, 15 nm × 15 nm), b-iii) high-resolution image with the corresponding chemical structure to show the bisacylperoxide connection of the linear polymer chains (−2 V, 5 pA, 5 nm × 5 nm). All images were obtained on Au(111).

functionalities. For the formation of Au–carboxylate branching, pre-orientation of the reacting moieties needs more space, which is fulfilled mainly in low-coverage areas of the surface.

The highly interesting acid coupling of the BDNA units to form the bisacylperoxide motif in the linear parts of these polymer chains was investigated further. The measurements revealed a naphthyl center-to-center distance of 1.08 ± 0.02 nm, which is too short for a metal carboxylate complex (calculated: 1.363 nm) or a connection of two acid functionalities via classical hydrogen bonding (calculated: 1.173 nm). DFT distance calculations for the suggested bisacylperoxide linkage (1.077 nm) between the BDNA units in the linear polymer sections are in excellent agreement with the experimentally measured distance. For better comparison all the distance values are given for the same conformation of the naphthyl units (for distances of the other conformers see Figure S5). Additionally, we calculated the DFT structures of a H-bonding dimer as well as two conformers of bis(2-naphthoyl) peroxide (BNP) on an Au surface (see Figure S2). The obtained distances agree well with those from the gas-phase calculations showing that the simpler gas-phase DFT calculations provide reliable values. Moreover, successful STM manipulations of BDNA polymer chains further supported the covalent nature of the linkage between the BDNA moieties (for further details see Figure S6).

To minimize the branching and to increase the reaction selectivity towards formation of linear bisacylperoxide-containing polymer chains, we repeated the experiment on an Au(100) substrate with channel structured surface topography. This defined topography should align the Glaser coupling product (BDNA) in the channels and subsequent polymerization via bisacylperoxide formation during the annealing to 130 °C should suppress branching. Indeed, the domino reaction of ENA on Au(100) provided nearly perfect linear polymers within the Au(100) channels with a chain length of up to over 100 nm (Figure 3c). We found these polymers to be thermally stable up to a temperature of 160 °C.

To further confirm the existence of the bisacylperoxide functionality between the BDNA units in these linear polymers, we synthesized, ex situ, various compounds containing two naphthyl groups with different potential linking entities (carboxylic acid anhydride, 1,2-diketone, or ethene moiety). These compounds were then deposited on the Au(111) surface and all systems showed a shorter naphthyl-to-naphthyl center-to-center distance. Moreover, also their contrast signatures in the STM data looked different, unambiguously revealing that these functionalities were not formed as linking moieties under the applied conditions (Figure S3). In addition, the BDNA molecule was ex situ prepared and sublimated to both Au(111) and Au(100) surfaces. Surprisingly, the STM images recorded directly after deposition revealed for both cases that the activation of the carboxyl function in the BDNA occurred already at room temperature and resulted in the formation of the same linear polymer chains observed in the ENA-high temperature experiments with a measured conjunction distance of 1.08 ± 0.02 nm between the naphthyl centers (Figure 4b,c). This result shows that the annealing temperature of 124 °C in our previous experiments with the ENA monomers was only needed to trigger the Glaser coupling process for formation of the BDNA units at the surface and not required for the O–O bond formation via dehydrogenative coupling. Since ENA itself does not dehydrogenate to give the corresponding peroxide at room temperature (see Figure 1a and Figure 2a), we assume that the BDNA structure bearing the butadiyne motive must provide this molecule unique properties, which seem to be essential for peroxide formation. This is further supported by the many examples on aromatic carboxylic acids adsorbed on Au surfaces not showing peroxide formation. Hence, the initial Glaser coupling activates the acid to undergo subse-

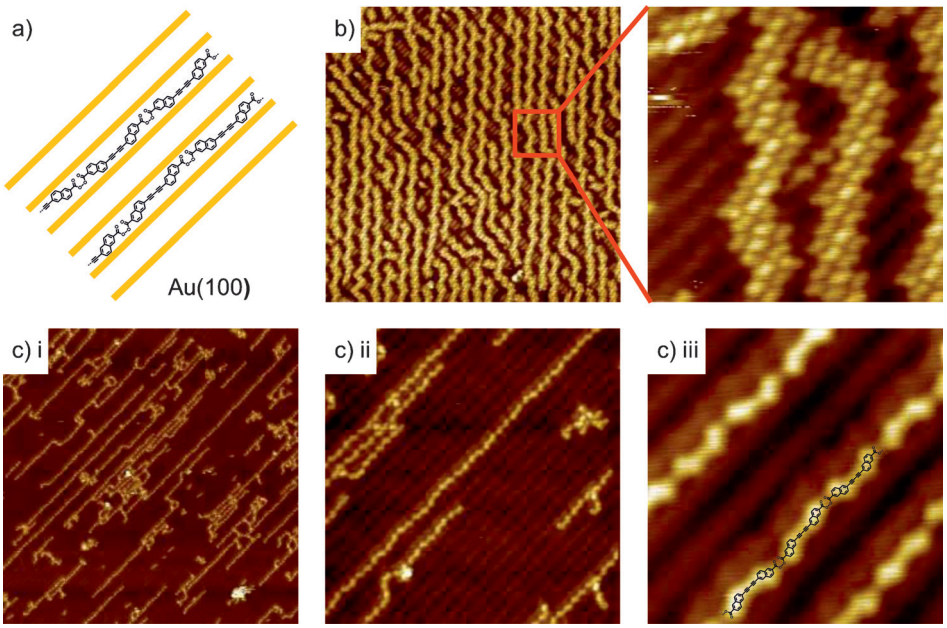

Figure 3. a) Illustration of the surface control on the polymerization. b) Overview STM image of the residual ENAs (−2 V, 10 pA, 80 nm×80 nm), with a close-up view (−2 V, 10 pA, 12.5 nm×12.5 nm). c) STM images of the reaction products after annealing at 130 °C, c-i) overview image (−1 V, 50 pA, 82 nm×82 nm). c-ii) STM image of a long bisacylperoxide polymer chain (−1 V, 50 pA, 30 nm×30 nm) and c-iii) high-resolution image with the corresponding chemical structure (−1 V, 50 pA, 8.4 nm×8.4 nm). All images were obtained on Au(100).

quent bisacylperoxide formation in a domino reaction. The activation mode is currently not understood.

To further experimentally confirm the existence of the bisacylperoxide linkage, we prepared, ex situ, bis(2-naphthoyl) peroxide (BNP) as a reference compound. The thermally labile BNP (decomposition at 146 °C) could be sublimated under UHV conditions at 120 °C onto Au(111) and the STM image revealed a surface covered with mainly intact BNP molecules (Figure 5b). Comparison of the STM images of the polymeric BDNA with the images of BNP revealed an excellent match of the measured conjunction distances (1.08 ± 0.02 nm) for these two systems. In addition, the contrast signature of the linkage entity in the images was also very similar. We also conducted a XPS analysis on both molecular layers (see the Supporting Information). The XPS data exhibit a very good correlation of poly-BDNA and the reference peroxide (BNP) further supporting the presence of the bisacylperoxide connection in the prepared polymer chains (Figure 5c). Furthermore, the XPS analysis of the Au–carboxylate coordination network shows only one O 1s component in the spectrum (see Figure S8), therefore an Au carboxylate complex can be excluded as the connection moiety in the poly-BDNA chains where two signals appear in the O 1s region.

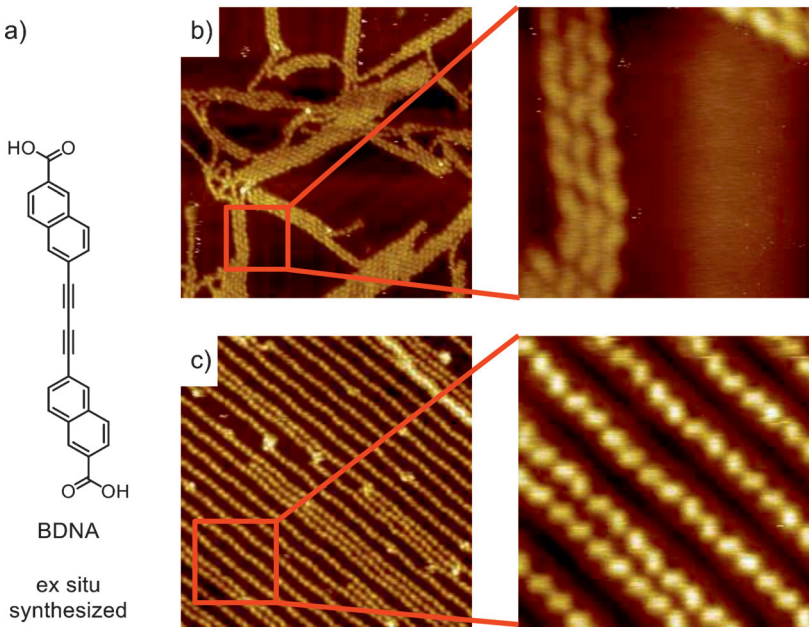

Figure 4. a) Structure of the ex situ synthesized BDNA. b) Overview STM image after deposition of the BDNA onto Au(111) (−0.5 V, 10 pA, 42 nm×42 nm), with a close-up view (−0.5 V, 10 pA, 8.4 nm×8.4 nm). c) Overview STM image after deposition of the BDNA onto Au(100) (−2 V, 10 pA, 42 nm×42 nm), with a close-up view (−1 V, 10 pA, 12 nm×12 nm).

In summary, we have presented on-surface dehydrogenative coupling of the carboxylic acid functionality in BDNA on two different gold surfaces, a reaction which is currently unknown in solution phase chemistry. By using this approach we were able to prepare linear bisacylperoxide connected polymer chains with a length of up to over 100 nm. This unprecedented on-surface reaction can be combined with a Glaser coupling step representing the first on-surface domino reaction sequence. This allows the readily accessible ENA to be used as a starting material for polymerization. We have found that the surface coverage influences reaction outcome. Formation of the bisacylperoxide functionality was verified by comparing STM images and XPS data with those obtained for an ex situ synthesized reference bisacylperoxide compound. The discovered dehydrogenative coupling of acids provides a valuable extension to the "reaction toolbox" for on-surface synthesis.

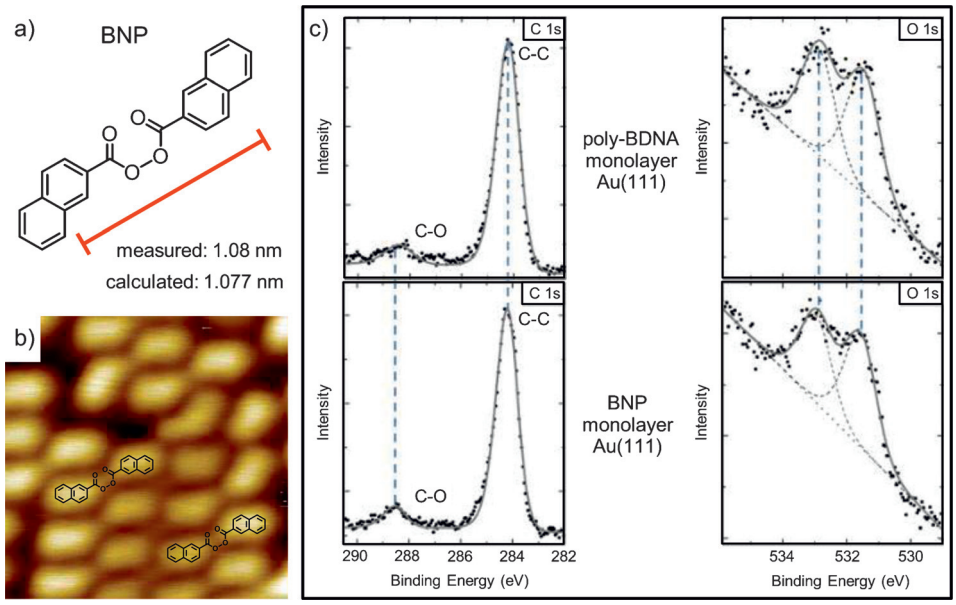

Figure 5. a) Structure of the ex situ synthesized BNP with its experimentally determined as well as the calculated naphthyl center-to-center distance. b) High-resolution STM image after deposition of the BNP onto Au(111) (−0.3 V, 10 pA, 4.2 nm×4.2 nm). c) XPS analysis of the bisacylperoxide formation, top: XPS data of the C 1s (peaks at 288.40 eV and 284.19 eV) and O 1s region (peaks at 532.86 eV and 531.45 eV) of a poly-BDNA monolayer on Au(111), bottom: XPS data of the C 1s (peaks at 288.52 eV and 284.19 eV) and O 1s region (peaks at 532.94 eV and 531.55 eV) of the reference compound BNP on Au(111).

Acknowledgments

We thank the Deutsche Forschungsgemeinschaft (SFB 858 and TRR61) for financial support. H.-Y.G. was supported by the Alexander von Humboldt Foundation.

Keywords: Glaser coupling · gold · scanning tunneling microscopy · self-assembly · surface chemistry

How to cite: *Angew. Chem. Int. Ed.* **2016**, *55*, 9777–9782
Angew. Chem. **2016**, *128*, 9929–9934

[1] A. Gourdon, *Angew. Chem. Int. Ed.* **2008**, *47*, 6950–6953; *Angew. Chem.* **2008**, *120*, 7056–7059.
[2] D. F. Perepichka, F. Rosei, *Science* **2009**, *323*, 216–217.
[3] C.-A. Palma, P. Samorì, *Nat. Chem.* **2011**, *3*, 431–436.
[4] J. Sakamoto, J. von Heijst, O. Lukin, A. D. Schlüter, *Angew. Chem. Int. Ed.* **2009**, *48*, 1030–1069; *Angew. Chem.* **2009**, *121*, 1048–1089.
[5] J. W. Colson, W. R. Dichtel, *Nat. Chem.* **2013**, *5*, 453–465.
[6] L. Grill, M. Dyer, L. Lafferentz, M. Persson, M. V. Peters, S. Hecht, *Nat. Nanotechnol.* **2007**, *2*, 687–691.
[7] L. Lafferentz, F. Ample, H. Yu, S. Hecht, C. Joachim, L. Grill, *Science* **2009**, *323*, 1193–1197.
[8] J. Cai, P. Ruffieux, R. Jaafar, M. Bieri, T. Braun, S. Blankenburg, M. Muoth, A. P. Seitsonen, M. Saleh, X. Feng, K. Müllen, R. Fasel, *Nature* **2010**, *466*, 470–473.
[9] R. Gutzler, H. Walch, G. Eder, S. Kloft, W. M. Heckl, M. Lackinger, *Chem. Commun.* **2009**, 4456–4458.
[10] M. O. Blunt, J. C. Russell, N. R. Champness, P. H. Beton, *Chem. Commun.* **2010**, *46*, 7157–7159.
[11] M. Bieri, M. T. Nguyen, O. Gröning, J. Cai, M. Treier, K. Aït-Mansour, P. Ruffieux, C. A. Pignedoli, D. Passerone, M. Kastler, K. Müllen, R. Fasel, *J. Am. Chem. Soc.* **2010**, *132*, 16669–16676.
[12] S. Weigelt, C. Busse, C. Bombis, M. M. Knudsen, K. V. Gothelf, T. Strunskus, C. Wöll, M. Dahlbom, B. Hammer, E. Lægsgaard, F. Besenbacher, T. R. Linderoth, *Angew. Chem. Int. Ed.* **2007**, *46*, 9227–9230; *Angew. Chem.* **2007**, *119*, 9387–9390.
[13] S. Weigelt, C. Busse, C. Bombis, M. M. Knudsen, K. V. Gothelf, E. Lægsgaard, F. Besenbacher, T. R. Linderoth, *Angew. Chem. Int. Ed.* **2008**, *47*, 4406–4410; *Angew. Chem.* **2008**, *120*, 4478–4482.
[14] L. Jiang, A. C. Papageorgiou, S. Cheol Oh, Ö. Sağlam, J. Reichert, D. A. Duncan, Y.-Q. Zhang, F. Klappenberger, Y. Guo, F. Allegretti, S. More, R. Bhosale, A. Mateo-Alonso, J. V. Barth, *ACS Nano* **2016**, *10*, 1033–1041.
[15] N. A. A. Zwaneveld, R. Pawlak, M. Abel, D. Catalin, D. Gigmes, D. Bertin, L. Porte, *J. Am. Chem. Soc.* **2008**, *130*, 6678–6679.
[16] M. Matena, T. Riehm, M. Stöhr, T. A. Jung, L. H. Gade, *Angew. Chem. Int. Ed.* **2008**, *47*, 2414–2417; *Angew. Chem.* **2008**, *120*, 2448–2451.
[17] F. Bebensee, C. Bombis, S.-R. Vadapoo, J. R. Cramer, F. Besenbacher, K. V. Gothelf, T. R. Linderoth, *J. Am. Chem. Soc.* **2013**, *135*, 2136–2139.
[18] O. Díaz Arado, H. Mönig, H. Wagner, J.-H. Franke, G. Langewisch, P. A. Held, A. Studer, H. Fuchs, *ACS Nano* **2013**, *7*, 8509–8515.
[19] H. Zhou, J. Liu, S. Du, L. Zhang, G. Li, Y. Zhang, B. Z. Tang, H.-J. Gao, *J. Am. Chem. Soc.* **2014**, *136*, 5567–5570.
[20] M. Abel, S. Clair, O. Ourdjini, M. Mossoyan, L. Porte, *J. Am. Chem. Soc.* **2010**, *132*, 1203–1205.
[21] M. In't Veld, P. Iavicoli, S. Haq, D. B. Amabilino, R. Raval, *Chem. Commun.* **2008**, 1536–1538.
[22] H.-Y. Gao, H. Wagner, D. Zhong, J.-H. Franke, A. Studer, H. Fuchs, *Angew. Chem. Int. Ed.* **2013**, *52*, 4024–4028; *Angew. Chem.* **2013**, *125*, 4116–4120.
[23] H.-Y. Gao, D. Zhong, H. Mönig, H. Wagner, P. A. Held, A. Timmer, A. Studer, H. Fuchs, *J. Phys. Chem. C* **2014**, *118*, 6272–6277.
[24] Q. Sun, C. Zhang, H. Kong, Q. Tan, W. Xu, *Chem. Commun.* **2014**, *50*, 11825–11828.
[25] Q. Sun, L. Cai, Y. Ding, L. Xie, C. Zhang, Q. Tan, W. Xu, *Angew. Chem. Int. Ed.* **2015**, *54*, 4549–4552; *Angew. Chem.* **2015**, *127*, 4632–4635.
[26] D. Zhong, J.-H. Franke, S. K. Podiyanachri, T. Blömker, H. Zhang, G. Kehr, G. Erker, H. Fuchs, L. Chi, *Science* **2011**, *334*, 213–216.
[27] M. Treier, N. V. Richardson, R. Fasel, *J. Am. Chem. Soc.* **2008**, *130*, 14054–14055.
[28] A. C. Marele, R. Mas-Ballesté, L. Terracciano, J. Rodríguez-Fernández, I. Berlanga, S. S. Alexandre, R. Otero, J. M. Gallego, F. Zamora, J. M. Gómez-Rodríguez, *Chem. Commun.* **2012**, *48*, 6779–6781.
[29] O. Díaz Arado, H. Mönig, J.-H. Franke, A. Timmer, P. A. Held, A. Studer, H. Fuchs, *Chem. Commun.* **2015**, *51*, 4887–4890.

[30] B. Yang, J. Björk, H. Lin, X. Zhang, H. Zhang, Y. Li, J. Fan, Q. Li, L. Chi, *J. Am. Chem. Soc.* **2015**, *137*, 4904 – 4907.
[31] A. Dmitriev, N. Lin, J. Weckesser, J. V. Barth, K. Kern, *J. Phys. Chem. B* **2002**, *106*, 6907 – 6912.
[32] S. Clair, S. Pons, A. P. Seitsonen, H. Brune, K. Kern, J. V. Barth, *J. Phys. Chem. B* **2004**, *108*, 14585 – 14590.
[33] D. Payer, A. Comisso, A. Dmitriev, T. Strunskus, N. Lin, C. Wöll, A. DeVita, J. V. Barth, K. Kern, *Chem. Eur. J.* **2007**, *13*, 3900 – 3906.
[34] A. P. Seitsonen, M. Lingenfelder, H. Spillmann, A. Dmitriev, S. Stepanow, N. Lin, K. Kern, J. V. Barth, *J. Am. Chem. Soc.* **2006**, *128*, 5634 – 5635.
[35] C. S. Kley, J. Čechal, T. Kumagai, F. Schramm, M. Ruben, S. Stepanow, K. Kern, *J. Am. Chem. Soc.* **2012**, *134*, 6072 – 6075.
[36] J. Čechal, C. S. Kley, T. Kumagai, F. Schramm, M. Ruben, S. Stepanow, K. Kern, *Chem. Commun.* **2014**, *50*, 9973 – 9976.
[37] H.-Y. Gao, P. A. Held, M. Knor, C. Mück-Lichtenfeld, J. Neugebauer, A. Studer, H. Fuchs, *J. Am. Chem. Soc.* **2014**, *136*, 9658 – 9663.
[38] L. F. Tietze, U. Beifuss, *Angew. Chem. Int. Ed. Engl.* **1993**, *32*, 131 – 163; *Angew. Chem.* **1993**, *105*, 137 – 170.
[39] L. F. Tietze, *Chem. Rev.* **1996**, *96*, 115 – 136.

Received: March 22, 2016
Published online: July 13, 2016

